Journal of Solid State Chemistry 187 (2012) 208–210

Contents lists available at SciVerse ScienceDirect

Journal of Solid State Chemistry

journal homepage: www.elsevier.com/locate/jssc

Structural analysis of Li-intercalated hexagonal boron nitride

A. Sumiyoshi [a,*], H. Hyodo [b], K. Kimura [a]

[a] Department of Advanced Materials Science, The University of Tokyo, Kiban-toh 502, 5-1-5 Kashiwanoha, Kashiwa-shi, Chiba, 277-8561, Japan
[b] Department of Materials Science and Technology, Tokyo University of Science, 2641 Yamazaki, Noda, Chiba 278-8510, Japan

ARTICLE INFO

Article history:
Received 7 October 2011
Received in revised form
29 December 2011
Accepted 1 January 2012
Available online 20 January 2012

Keywords:
Hexagonal boron nitride
Intercalation
Lithium
X-ray diffraction

ABSTRACT

A structural investigation of Li-intercalated hexagonal boron nitride (Li-h-BNIC) was performed by synchrotron powder X-ray diffraction analysis and transmission electron microscopy. The host BN framework of Li-h-BNIC was expanded by Li-intercalation. The intralayer B–N bond length was increased by 2.48(1)% and the interlayer distance was expanded by 12.86(1)%. No superlattice structure of intercalated Li was observed.

1. Introduction

Hexagonal boron nitride (h-BN) has a graphitelike honeycomb layered structure. Compared with graphite, h-BN is a wide band gap semiconductor and its interlayer interaction is stronger than that of graphite because of its partial ionic characteristics originating from the charge transfer from N to B. Recently, h-BN single crystal has been synthesized by a high-temperature and high-pressure process, and the ultraviolet luminescence has been experimentally observed from the 5.8 eV direct exciton transition of h-BN [1].

Graphite intercalation compounds (GICs) have been widely studied [2] in terms of their structure and properties. Alkali–metal GICs exhibit metallization and superconductivity [2,3]. It is thought that intercalation into an h-BN interlayer is difficult because of the strong interlayer interaction originating from the partial ionic characteristic of the interlayer B–N bond.

Several experimental studies on h-BN intercalation compounds (h-BNICs) have been reported [4–8]. However, successful and clear intercalation has been seldom achieved. Shen et al. [4] succeeded in the synthesis of SO_3F–h-BNIC and reported its metallic electrical conductivity and the increase in interlayer distance upon intercalation.

On the theoretical side, some first-principles calculations have predicted the possibility of alkali–metal h-BNICs with metallic characteristics [9–11].

Altintas et al. [11] mentioned the necessity of external pressure to synthesize Li-h-BNIC because of its positive formation enthalpy compared with that of pristine Li and h-BN. In contrast, it has been experimentally shown that the formation enthalpy of Li GICs is negative, which was also confirmed in their calculation [11]. The positive formation enthalpy of Li-h-BNIC is consistent with the difficulty of synthesizing Li-h-BNIC and other h-BNICs.

From another viewpoint, Oba et al. [12] reported the possibility of inducing an impurity level in the wide band gap of h-BN by the "dilute" intercalation of donor alkali metal atoms and acceptor F atom. The comparison of h-BNICs formed by dilute and "concentrated" intercalation into h-BN is also of interest.

We succeeded in the intercalation of Li into h-BN under more reactive experimental conditions than those in previous studies on the synthesis of alkali-metal-h-BNICs [13]. In this study, we investigated the structure of the obtained Li-h-BNIC compound by synchrotron radiation powder X-ray diffraction (XRD) analysis and transmission electron microscopy (TEM).

2. Experimental

h-BN powder and Li metal were set in a BN or Ta crucible under an Ar atmosphere in a glove box and the crucible was sealed in a stainless steel tube by arc welding. The sealed crucible was annealed at 1523 K for 10 h. The synthesis of the Li-h-BNIC phase was verified by powder XRD analysis with Cu-*Ka* radiation (Rigaku RINT-2000). The sample was then investigated by synchrotron radiation powder XRD analysis (Spring-8 BL02B2) and TEM (JEM-4000FX II). The obtained Li-h-BNIC was set in Lindemann glass capillaries (0.3 mm diameter, Hilgenberg). The X-ray wavelength was calibrated by the measurement of CeO_2. The calibrated wavelength was 0.8028 Å. The XRD patterns were analyzed by the Rietveld method using the RIETAN-2000 program [14].

* Corresponding author. Fax: +81 04 7136 3761.
E-mail address: sumiyoshi@phys.mm.t.u-tokyo.ac.jp (A. Sumiyoshi).

0022-4596/$ - see front matter © 2012 Elsevier Inc. All rights reserved.
doi:10.1016/j.jssc.2012.01.002

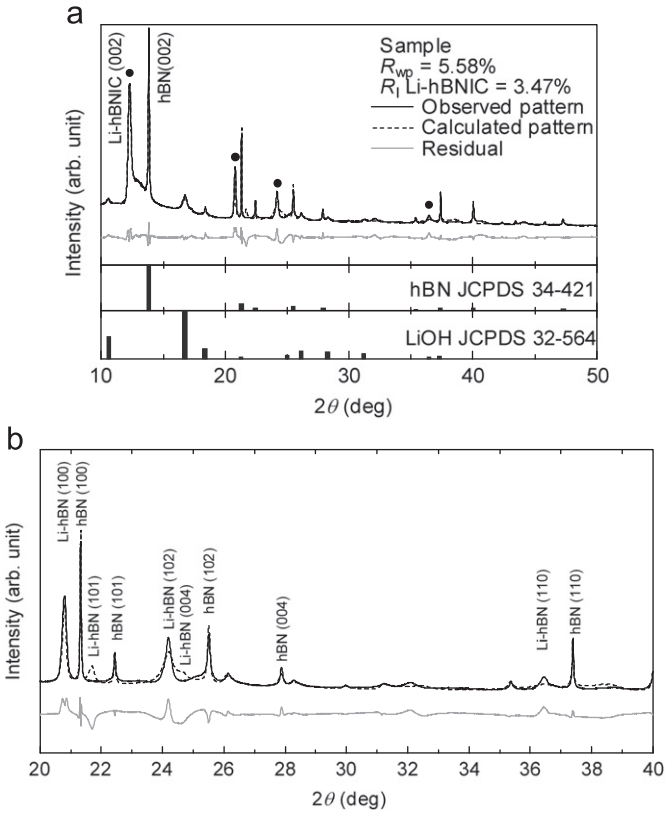

Fig. 1. (a) XRD pattern and fitting result of the sample. The black line is the observed pattern, the dashed line is the calculated pattern, and the gray line is the residual between the observed pattern and the calculated pattern. Dotted peaks are peaks of the Li-h-BNIC compound. (b) Magnified sample pattern. 2θ is from 20 to 40°.

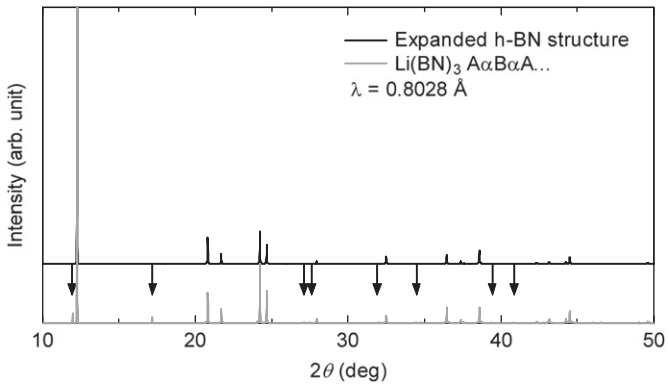

Fig. 2. Simulated XRD pattern of expanded h-BN lattice model and Li(BN)$_3$ model with AαBαA… stacking. Peaks originating from Li are indicated by arrowheads.

3. Results and discussion

Fig. 1 shows the XRD pattern of the present sample and the result of Rietveld fitting. The main phases are Li-h-BNIC, pristine h-BN, and LiOH. Although the signature of $LiOHH_2O$ is also observed, even the strongest peak of this phase, which appears at 17.3°, has very weak intensity and is difficult to see in Fig. 1. Because of these weak intensities, $LiOHH_2O$ was considered to be absent in the subsequent analysis. LiOH and $LiOHH_2O$ are considered to have been produced when the sample was exposed to the air during the experimental procedure.

In the *c* direction, a strong (0 0 2) diffraction peak corresponding to an interlayer distance of Li-h-BNIC 3.76 Å was observed at 12.27°. Compared with the (0 0 2) diffraction peak of pristine h-BN at 22.67°, which indicates an h-BN interlayer distance of 3.33 Å, the expansion ratio of the BN interlayer distance compared with that before Li intercalation is 13(1)%. This expansion ratio is similar to that in a previous report on analysis by XRD in a laboratory [13]. In the *a* direction, uncharacterized diffraction peaks are observed at 20.81° and 24.22°, which are located at lower angles than those of h-BN (1 0 0) and (1 0 2) at 21.33° and 25.51°, respectively. These diffraction peaks were assumed to indicate the expansion in the *a* direction of the host h-BN lattice. The assumed B–N bond length in the *a* direction is 1.48 Å, which is also greater than 1.45 Å for h-BN. Then Rietveld fitting was performed using the assumed expanded host h-BN lattice model for the structure of Li-h-BNIC. The obtained R_{wp} and R_I were 5.58% and 3.47%, respectively. Because of these relatively low *R* factors, the uncharacterized peaks were able to be fitted by the expanded h-BN lattice model. In the case of alkali- and alkaline earth metal GICs, the intercalant is arranged periodically between the graphite interlayers, and the GICs from superlattice structures. If Li-h-BNIC also forms a superlattice structure, it can be confirmed by synchrotron radiation XRD with a high S/N ratio. Fig 2 shows the simulated XRD pattern of the Li(BN)$_3$ with is AαBαA…stacking, which has the same arrangement of Li as LiC_6 for simplicity. New peaks can be observed, which are attributed to the periodicity of the intercalated Li atoms. However, no superlattice diffraction was observed in the experimentally obtained XRD patterns. Considering that the host BN lattice remains, a random Li arrangement is concluded. According to Kambe et al. [15], the Li arrangement of the *stage-1* GIC LiC_6 changes with temperature and an irreversible order-to-disorder transition occurs at a high temperature. Therefore, Li-h-BNIC with an ordered Li arrangement might also be synthesized by a suitable synthesis method under appropriate conditions.

Some contradictions remain between the observed pattern and the pattern of the expanded h-BN lattice model. If Li-h-BNIC has a simply expanded h-BN lattice structure, a (1 0 1) diffraction peak at 21.71° and a (0 0 4) diffraction peak at 24.65° should appear, similarly to those for pristine h-BN. However, the (1 0 1) and (0 0 4) diffraction peaks of the expanded h-BN lattice model did not appear in the experimentally observed pattern. In addition, although the (0 0 2), (1 0 0), and (1 1 0) diffraction peaks of Li-h-BNIC were fitted by the expanded h-BN lattice model, the peaks were broadened and their half widths at half maximum were about three times greater than those of pristine h-BN. These findings indicate that some structural disorder was induced into the host h-BN structure by Li intercalation.

Fig 3 shows the TEM electron diffraction patterns of the pristine h-BN and Li-h-BNIC samples. Superlattice diffraction was not observed. The diffraction pattern became Debye–Scherrer-ring-like, although sixfold symmetry remained. This existence of sixfold symmetry in the electron diffraction pattern and *a*-direction, (1 0 0) and (1 1 0) diffraction peaks in the XRD pattern imply that the host h-BN atomic layer structure remained after Li intercalation. Furthermore, it is speculated that rotational disordered stacking of the sixfold hBN atomic layer explains the sixfold symmetry remaining in the Debye–Scherrer-ring-like diffraction pattern. This turbostratic BN layer stacking may arise from the weakened interaction between neighboring BN layers caused by the increase in interlayer distance due to Li intercalation. It is still not clear whether this turbostratic BN layer stacking is intrinsic for Li-h-BNIC or is due to the existence of moisture during the experimental procedure.

Table 1 shows the experimentally determined intralayer and interlayer bonding distances for pristine h-BN, the present Li-h-BNIC, pristine graphite [16], LiC_6 [17], and LiC_3 [18], and theoretically calculated values [11]. The expansion ratio of the Li-h-BNIC intralayer bond length is markedly larger than those of donor-type alkali-metal GICs (LiC_6 and LiC_3), although that of the interlayer distance is

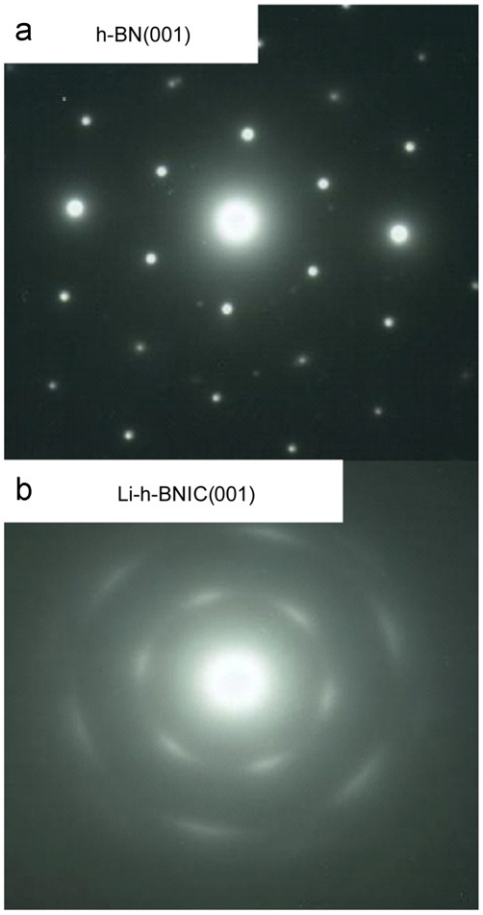

Fig. 3. TEM electron diffraction patterns of (a) pristine hBN and (b) Li-h-BNIC.

Table 1
Intralayer distances, interlayer distances, and expansion ratios of host phases before and after Li intercalation. d_a is the intralayer C–C and B–N bond distance. d_c is the interlayer distance.

Compounds	d_a (Å)	d_c (Å)	$\Delta d_a/d_{a0}$ (%)	$\Delta d_c/d_{c0}$ (%)
Exp.				
h-BN	1.4454(1)	3.3315(1)	–	–
Li-h-BNIC	1.4813(1)	3.7599(3)	2.48(1)	12.86(1)
Graphite [16]	1.423(1)	3.356(2)	–	–
LiC_6 [17]	1.435(1)	3.705(1)	0.85(1)	10.4(1)
LiC_3 [18]	1.43	3.70	0.49(1)	10.3(1)
Calc. [11]				
h-BN	1.440	3.256	–	–
$Li(BN)_3$	1.455	3.940	1.0	21.0
$Li_4(BN)_6$	1.485	3.717	3.1	14.2
Graphite	1.408	3.328	–	–
LiC_6	1.425	3.857	1.2	15.9
LiC_3	1.453	3.667	3.2	10.2

similar to those of the GICs. Pietronero and Strassler [19] revealed the relation between C–C bond distance and charge transfer for several intercalant concentrations of donor-type alkali-metal GICs and accepter-type metal halide GICs. In the case of alkali–metal GICs, the expansion ratio of the intralayer bond length is explained by the degree of charge transfer from the intercalant to the host graphite layer. A larger intralayer expansion ratio of Li-h-BNIC may indicate a larger charge transfer from the intercalant Li to the host BN layer. Compared with the calculation by Altintas et al. [11], it is consistent that the *a*-direction intralayer B–N bond lengths of pristine h-BN and Li-h-BNIC are larger than those of C–C pristine graphite and the Li GIC. The present observed expansion ratios for both the *a* and *c* directions of Li-h-BNIC are similar to those of $Li_4(BN)_6$ than $Li(BN)_3$. However, note that for the Li GIC, the theoretically calculated *a*-direction expansion ratio of LiC_3 is not consistent with the experimentally observed value, although the calculated and experimentally observed *c*-direction expansion ratio of LiC_3 and these in both directions for LiC_6 are consistent. The origin of this discrepancy for the *a*-direction expansion ratio of LiC_3 may be due to the different positions of intercalant Li atoms, because atoms are considered to exist either above or below the interlayer horizontal plane in the experimental results but such a division may not be considered in the structure model used in the calculation study. Therefore, it is not yet clear whether or not the agreement between the intralayer B–N distance calculated by Altintas et al. [11] and the present observed value is reasonable. Further investigation is needed to clarify the origin of the large expansion ratio of the Li-h-BNIC intralayer B–N distance.

4. Conclusions

The expansion of the host h-BN intralayer B–N bond and the interlayer distance in Li-intercalated h-BN was observed by synchrotron radiation powder XRD analysis. A large charge transfer from the intercalant Li to the host BN layer is indicated by the considerably larger intralayer bond expansion than those of alkali-metal GICs. No superlattice structure of the intercalant Li was observed at room temperature by XRD and TEM. This indicates the random arrangement of the intercalant Li and turbostratic BN stacking caused by Li intercalation.

Acknowledgments

One of the authors (A. S.) was supported by a Research Fellowship for Young Scientists from Japan Society for the Promotion of Science. The synchrotron radiation experiments were performed at the BL02B2 station of SPring-8 with the approval of Japan Synchrotron Radiation Research Institute (Proposal No. 2009A1325). The TEM observation was technically supported by Mr. H. Tsunakawa, and Mr. T. Itoh, Institute of Engineering Innovation, The University of Tokyo. This work was partly supported by Scientific Research on Priority Areas of New Materials Science Using Regulated Nano Spaces, KAKENHI No. 19051005 from MEXT.

References

[1] K. Watanabe, T. Taniguchi, H. Kanda, Nat. Mater. 3 (2004) 404.
[2] M.S. Dresselhaus, G. Dresselhaus, Adv. Phys. 51 (2002) 1.
[3] N. Emery, C. Hérold, M. D'Astuto, V. Garcia, Ch. Bellin, J. Marêché, P. Lagrange, G. Loupias, Phys. Rev. Lett. 95 (2005) 1.
[4] C. Shen, S.G. Mayorga, R. Biagioni, C. Piskoti, M. Ishigami, A. Zettl, N. Bartlett, J. Solid State Chem. 147 (1999) 74.
[5] M. Sakamoto, J.S. Speck, M.S. Dresselhaus, J. Mater. Res. 1 (1986) 685.
[6] G.L. Doll, J.S. Speck, G. Dresselhaus, M.S. Dresselhaus, J. Appl. Phys. 66 (1989) 2554.
[7] A.G. Freeman, J.P. Larkindale, Inorg. Nucl. Chem. Lett. 5 (1969) 937.
[8] E. Budak, C. Bozkurt, J. Solid State Chem. 177 (2004) 1768.
[9] B.L. Faifel, L.A. Gribov, A.O. Domitrinenko, A.F. Bol'shakov, Sov. Phys. Crystallogr. 31 (1985) 497.
[10] S. Okada, M. Otani, Phys. Rev. B 81 (2010) 3.
[11] B. Altintas, C. Parlak, C. Bozkurt, R. Eryiğit, Eur. Phys. J. B 79 (2011) 301.
[12] F. Oba, A. Togo, K. Watanabe, T. Taniguchi, Phys. Rev. B 81 (2010) 20.
[13] A. Sumiyoshi, H. Hyodo, K. Kimura, J. Phys. Chem. Solids 71 (2010) 569.
[14] F. Izumi, T. Ikeda, Mater. Sci. Forum 321-324 (2000) 198.
[15] N. Kambe, M.S. Dresselhaus, G. Dresselhaus, S. Basu, A.R. Mcghie, J.E. Fischer, Mater. Sci. Eng. 40 (1979) 1.
[16] P. Trucano, R. Chen, Nature 258 (1975) 136.
[17] D. Guerard, A. Herold, Carbon 13 (1975) 337.
[18] D. Guerard, R. Janot, J. Phys. Chem. Solids 65 (2004) 147.
[19] L. Pietronero, S. Strassler, Phys. Rev. Lett. 47 (1981) 593.